

Supporting Information

Proton conduction through oxygen functionalized few-layer graphene

Chanderpratap Singh[†], Nikhil S[†], Anwasha Jana[†], Ashish Kumar Mishra^{#*} and Amit Paul^{†*}

[†]Department of Chemistry, [#]Department of Physics, Indian Institute of Science Education and Research (IISER) Bhopal, Madhya Pradesh, India 462066.

Figure/ Table	Content	Page No.
	Materials used and characterization	S2-S3
	Synthesis of OFG (150)	S3-S4
	Experimental details of Proton conductivity measurement, Experimental details of supercapacitor studies, Electrical conductivity, Powder X-ray diffraction analysis and PXRD pattern of Graphite (150 micron)	S4-S7
Figure S1, Figure S2a, Figure S2b and S3	PXRD pattern of Graphite (150 micron), Full scan XPS Spectra of OFG (150), O 1s spectra of OFG (150) and GO (150) and related discussion	S7-S8
Figure S4 and S5	TGA of OFG (150), and GO (150), Raman spectra of OFG (150) and GO (150) and discussion related to Raman spectra	S9
Figure S6, S7	BET profile of OFG (150), Discussion related to BET study, Water uptake measurement of OFG (150).	S10
Figure S8, S9 and S10	Water uptake measurement of GO (150), Time dependent proton conductivity of OFG (150) and PXRD pattern of OFG (150) at different temperature with 95% RH	S11
Figure S11	Supercapacitor results of OFG (150) Discussion related to supercapacitor studies.	S12-S13
Figure S12, Table S1	Fitted data of EIS plot of proton conductivity. PXRD results.	S13
Table S2a, S2b, S2c,	XPS results.	S14
Table S3, Table S4, Table S5,	Comparison of proton conductivity values with literature, Comparison of	S15-S16

Table S6	proton conductivity results before and after thermal annealing, Proton conductivity at different temperature 95% RH, Specific capacitance values and references	
----------	---	--

Material used:

Graphite (particle size 150 micron, Cat# 496588), concentrated sulfuric acid (Cat# 320501), *N*-methyl-2-pyrrolidone (NMP), poly(vinylidene fluoride) (PVDF), potassium bromide, and barium chloride solution were purchased from Sigma-Aldrich. Platinum (Pt) foil and Pt wire were purchased from Alfa Aesar. Standard calomel electrode (SCE) was purchased from CH Instruments, TX, USA. Hydrogen peroxide (50%) and potassium permanganate were purchased from Rankem, India and Fischer Scientific respectively. Formic acid (Cat#CE5C650198) and acetone were purchased from Merck and Spectrochem, India respectively. Milli-Q water (> 18 MΩ.cm) was used during all the synthesis.

Characterization:

The powder X-ray diffraction (PXRD) patterns were recorded by Bruker AXS D8 Advance with Cu K α radiation (1.54 Å) with a step size of 0.02° in a 2 θ range of 0- 60°. Thermal gravimetric analysis (TGA) was performed by Perkin Elmer TGA 4000 instrument in a temperature range from 30-900 °C at a scan rate of 10 °C/min with a N₂ flow rate of 10 mL/min. For morphological studies, dried samples were spread over carbon tape and gold coated for 120 s, and scanning electron microscopy (SEM) studies were performed using Carl ZEISS (ultraplus) FE-SEM at 20 kV. Transmission electron microscopy (TEM, FEI TECNAI G² S-Twin) experiments were performed under an accelerating voltage of 200 kV. TEM samples were prepared by drop casting the suspension of the sample (0.5 mg in 15 mL isopropanol) onto a carbon-coated copper grid and solvent was evaporated under ambient conditions overnight. The Raman spectroscopy experiments were performed by Lab RAM HR 800 (HORIBA) with exciting wavelength of 632.8 nm. Nitrogen adsorption/desorption experiments were performed on Quantachrome Autosorb QUA211011 equipment for surface area measurements. Samples were degassed under high vacuum at 150 °C for 24 h. Water adsorption/desorption experiments were performed for degassed powdered sample (OFG (150) at 150 °C for 24 h, GO (150) at 80 °C for 24 h) in the vapour state using a BELSORP-aqua3 (BEL Japan) volumetric or gravimetric analyzer. FT-IR spectra were collected using Perkin Elmer spectrum BX spectrophotometer using pellets of samples with KBr. Electrical conductivity measurements were carried on physical property measurement system (PPMS, Model 6000) Quantum Design, USA. Dynamic light scattering (DLS) measurements were performed on dilute solution for which 1 mg of active material in 20

ml of isopropanol was mildly sonicated for half an hour. Thereafter, supernatant were collected after 6 h for measurement by using Delsa™ Nano (Beckman Coulter) instrument at 25 °C using CONTIN algorithm. Electrochemical experiments were carried out using CH Instruments, Austin, TX bipotentiostat (Model CHI 760D), potentiostat (Model CHI 620E) and BioLogic instrument model (SP300). Capacitance measurements were performed using cyclic voltammetry, galvanostatic charge/discharge and electrochemical impedance spectroscopy (EIS) techniques with a regular three electrodes cell. The proton conductivities of samples were measured by using a quasi-four-probe method using a solarton SI 1260 Impedance/Gain-Phase Analyzer and 1296 Dielectric Interface with in the frequency range of 1 Hz to 1 MHz. The temperature and humidity were controlled by programmable incubator (JEIOTECH, TH- PE series). The XPS experiment were performed on vacuum dried powder sample with drop size of (1.5 mm radius) on sample holder, by using PHI 5000 Versa Prob II, FEI Inc. with scan time one hour per element for Core level scan (Energy band of 20 eV, with Pass setting of 23.5 eV, 0.025 eV Step, 100 ms time per step, 5 cycles).

Synthesis of OFG (150):

Graphite oxide (GO) was prepared using a modified Hummer's method. Graphite (particle size 150 micron) (2.5 gm) was first sonicated in acetone for 30 min. Thereafter, graphite was filtered through a sintered glass filter and dried in an oven at 60 °C for 2 h. **Graphite (2 gm) was suspended in 138 mL (2.6 mole) conc. sulfuric acid in an ice bath (0 °C) in a 250 mL round bottom flask equipped with a magnetic stir bar. 12 gm of KMnO_4 (75 mmole) was then added cautiously covering a time span of approximately 30 min so that the temperature of the solution did not exceed 20 °C. The solution was then stirred at 35 °C using a reflux condenser for 12 h. Extra amount of acid has been used because of following reasons: (a) acid catalyzed hydrolysis of epoxide to produce more hydroxyl group, and (b) excess acid helps in increasing the reactivity of MnO_4^- as an oxidizing agent.**¹ After that, 92 mL of distilled water was added and stirring continued for an additional period of 30 min, during this step temperature will reach 55 °C. Then the content was poured into 280 mL of distilled water and 10 mL of 50% hydrogen peroxide was added to destroy the excess KMnO_4 . The complete removal of KMnO_4 was indicated by a color change from dark to yellow. GO was then isolated by a sintered glass filter and washed with copious amount of water (500 ml). Washing was continued until sulphate was no longer detected in the filtrate which was confirmed by addition of barium chloride solution in the filtrate. **Thereafter, filtrate was washed with 30 ml of formic acid solution (30 %) to intercalate formic acid in the inter-lamellar region of GO and dried in an oven at 60 °C for 24 h.**

Prepared GO was named as GO (150) where the numeric 150 indicates the particle size of parent graphite precursor purchased from Sigma-Aldrich. After drying, GO samples were stored in vials at ambient conditions. For GO reduction, 0.5 gm of prepared GO was poured in a 500 ml conical flask. Thereafter, conical flask was kept inside the preheated hot air oven at 160 °C for **8 min to complete the exfoliation process**. Oxygen functionalized few-layer graphene (OFG) material has been named as OFG (150). The bold sentences indicate the synthetic modification of this study from our previous studies (*RSC Adv.* 2014, **4**, 15138 and *J. Mater. Chem. A* 2015, **3**, 18557). **GO (150) used for characterization was prepared without formic acid washing.**

Full scan XPS spectrum revealed that OFG (150) was only consisting of carbon, oxygen (Figure S2a), hydrogen (not detectable by XPS) and devoid of any other elements. Furthermore, PXRD result revealed a peak at 10.9° corresponding to GO(150) was absent in OFG(150) (Figure 1a), indicating complete exfoliation of GO(150).

Experimental details of Proton conductivity measurement:

70 mg of as synthesized samples were finely grinded and then pressed in a pellet maker to obtain a uniform pellet of 1.3 – 1.5 mm thickness and 6 mm diameter at 4 tons of pressure. Before each experiment, initially samples were equilibrated for 5 hours and thereafter equilibrated for half an hour at each temperature and one hour at each humidity step. The resistance correspondence to the proton transfer was calculated by fitting the semicircle of Nyquist plot. The proton conductivity was calculated by using the equation, $\sigma = L / (RA)$, where, σ = proton conductivity, L= thickness of the pellet, R = resistance, A = area of the pellet (πr^2 , r = radius of pellet). Activation energies were determined from the slope of Arrhenius plots.

Experimental Details of Supercapacitor Studies:

Saturated calomel electrode (SCE), Pt wire, and OFG coated Pt foil were used as reference, counter, and working electrode, respectively. For supercapacitor studies, platinum (Pt) foils were coated with OFG (active material). For fabrication purpose, first Pt foils were cleaned in acetone by sonication for half an hour and dried in air. After that 1 ml N-methyl-2-pyrrolidone (NMP), 1 mg poly(vinylidene fluoride) (PVDF) binder, and 6 mg OFG were added. The solution mixture was stirred for 6 h to enhance the homogeneity of the solution. A 100 μ l of aliquot was drop casted and spreaded on an electrode covering 1 cm² area and dried

at 100 °C for 8 h in a hot air oven. The mass of material deposited on each electrode was 0.8 mg. Cyclic voltammetry (CV) experiments were performed in the potential range of -0.2 to 0.8 V versus SCE at various scan rates (1, 2, 5, 10, 20, 50 and 100 mV/s). Galvanostatic charge/discharge experiments were performed with in the cyclic potential range of -0.2 to 0.8 versus SCE at different current densities (0.5, 0.7, 0.8, 1, 2, 5 and 10 A/g). Electrochemical Impedance Spectroscopy (EIS) data has been collected at potential of 0 V bias over frequency range of 0.01-10⁵ Hz at amplitude of 0.01 V. By using eq. (1), capacitance values were calculated from cyclic voltammograms, where C , I , E and ν represent capacitance, current, potential window, and scan rate respectively. The numerator of this equation was calculated by integrating the area of cyclic voltammogram. Capacitances from galvanostatic charge/discharge curves were calculated using eq. (2), where t is the time taken to complete charge/discharge process. Specific capacitance values were calculated by dividing calculated capacitance by the weight of material deposited on electrodes.

$$C = \int (IdE)/(2 * E * \nu) \quad (1)$$

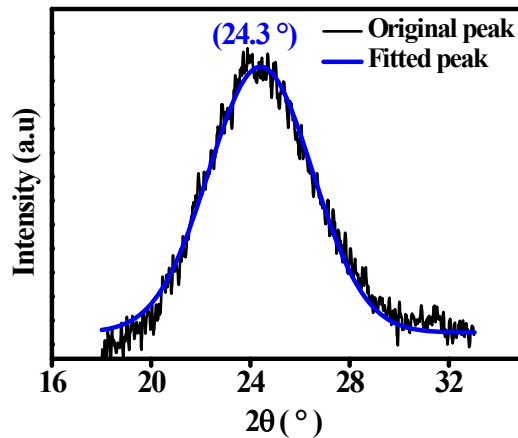
$$C = (I * t)/(2 * E) \quad (2)$$

Preparation of sample for electrical conductivity measurement:

For electrical conductivity measurement, OFG pellets were made by applying 4 tons force on 6 mm circular diameter pellet. Thereafter, pellets were cut in rectangular shapes. The dimensions were (thickness (0.09 cm), width (0.38 cm)). Probe spacing was fixed at 0.1 cm. Electrical Conductivity was calculated using formula as follows. (*Nat. Chem.* 2009, **1**, 403.)

$$\begin{aligned} \text{Conductivity (S/cm)} &= \frac{\text{probe spacing (cm)} \times \text{current (mA)}}{\text{Voltage (mV)} \times \text{width of film (cm)} \times \text{film thickness (cm)}} \\ &= 0.1(\text{cm})/0.38(\text{cm}) * 0.09(\text{cm}) * 25\Omega = 0.1 \text{ S/cm} \end{aligned}$$

XRD analysis using Scherrer equation for OFG (150):



Determination of d-

From Bragg's law

$$n\lambda = 2d\sin\theta$$

n is an integer

λ = wavelength of incident light

d = interlayer distance

θ = the angle between the incident ray and the scattering planes

Using, n = 1, $\lambda = 1.54 \text{ \AA}$, $2\theta = 24.3^\circ$, $\theta = 12.15^\circ$

$$d = 1.54 / (2 \times \sin(12.15)) = 3.6 \text{ \AA}$$

Determination of L_c and N-

From Scherrer formula,

$$L_c = (K\lambda) / (\beta \cos\theta)$$

L_c = Mean crystallite length along c-axis

K = dimensionless shape factor, typical value is 0.9 for L_c .

β = line broadening at full width half maxima in radian = 86×10^{-3}

β was determined by Voigt fitting

$\theta = 12.15 = 0.212$ radian

$\lambda = 0.154$ nm

Hence, $L_c = (0.90 \times 0.154) / (86 \times 10^{-3} \times \cos(0.212))$

$$L_c = 16.1 \text{ \AA}$$

N = Number of layers

$$N = 16.1 / 3.6 = 4-5 \text{ layers}$$

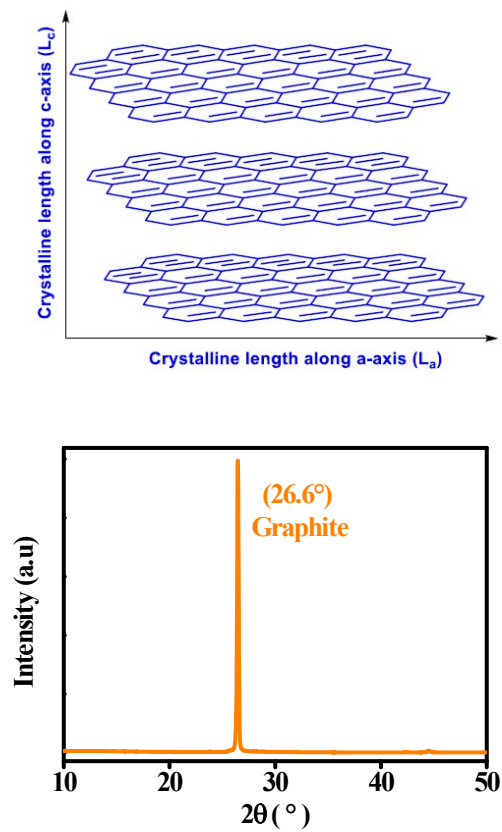


Figure S1: PXRD patterns of pristine Graphite (150 micron).

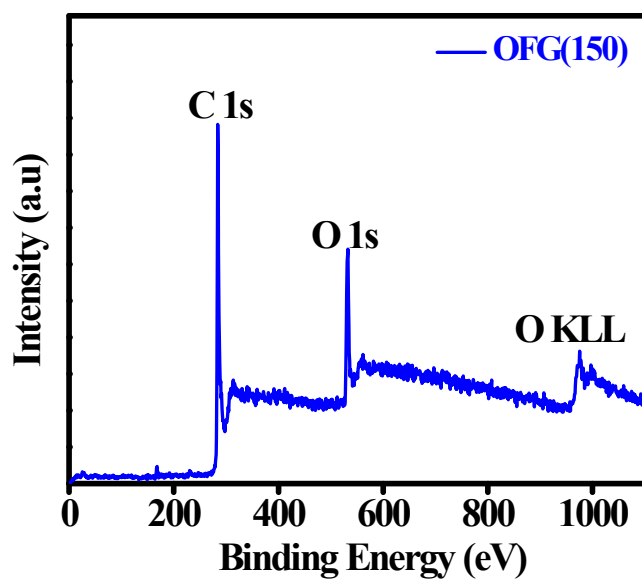


Figure S2a: Wide-scan XPS spectrum of OFG (150)

O 1s XPS spectra of OFG (150) and GO (150):

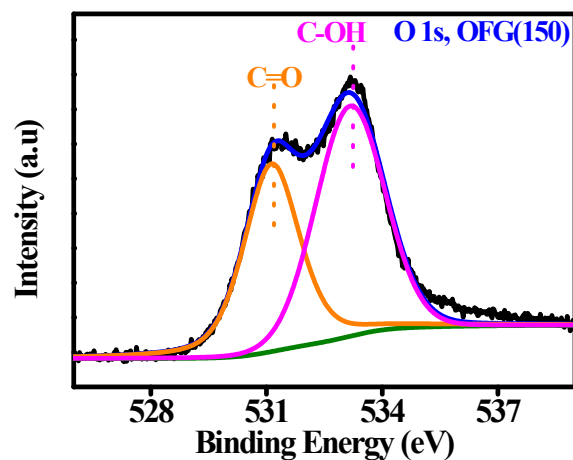


Figure S2b: O1s XPS spectrum of OFG (150).

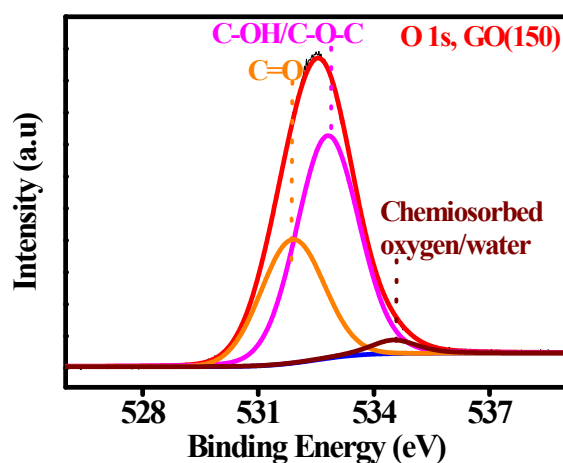


Figure S3: O1s XPS spectrum of GO (150).

Discussing on O 1s spectra: O 1s spectra of OFG (150) showed a peak at 533.1 eV corresponding to the presence of hydroxyl and absence of epoxy functionality² (Figure S2). In contrast, O 1s spectrum of GO (150) showed a peak at 532.8 eV which corresponds to both hydroxyl and epoxy³ (Figure S3). Besides, OFG (150) and GO (150) also showed a peak at 531.1 eV and 531.9 eV for ketone functionality⁴ (Figure S2, S3). GO (150) O 1s spectrum showed a peak at 534.5, which is correspondence to chemisorbed oxygen/water.³

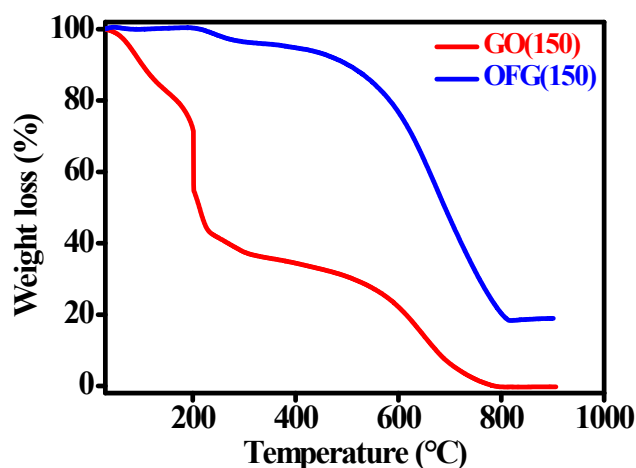


Figure S4: TGA traces of OFG (150) and GO (150).

Raman spectra of OFG (150) and GO (150):

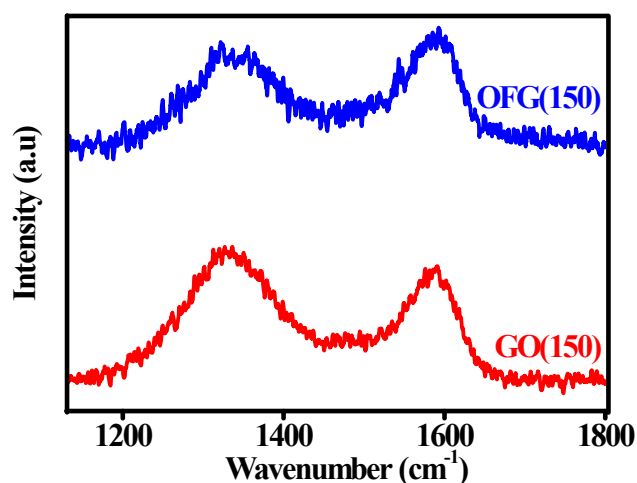


Figure S5: Raman spectra of OFG (150) and GO (150).

Discussing Related to Raman Spectra: Raman spectra for GO (150) and OFG (150) exhibited D (correspond to disorder) and G (correspond to in-plane vibration of C atoms) bands around 1330 and 1590 cm^{-1} respectively (Figure S5). The intensity ratios of these two bands (I_D/I_G) are measure of degree of disorder.⁵ Decreased ratio of I_D/I_G for OFG (150) compared to GO (150) was indicative of repairing of defects created during oxidation process.

N₂ adsorption/desorption isotherm of OFG (150):

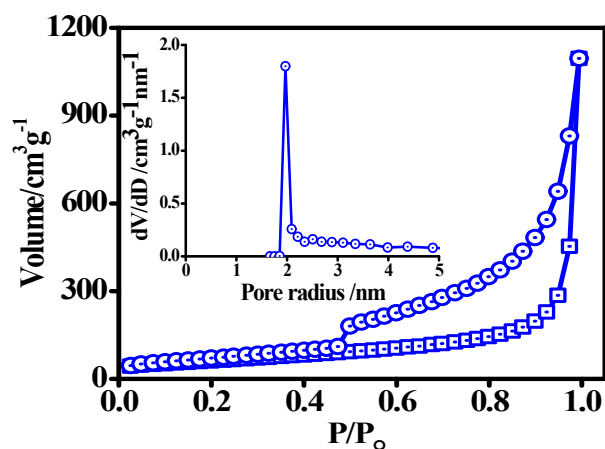


Figure S6: N₂ adsorption/desorption isotherm plot and BJH plot (inset) of pore size distribution for OFG (150).

Discussion related to BET study: N₂ adsorption/desorption profile for OFG (150) exhibited type-III/IV isotherm profile with hysteresis loop of H2 type (according to IUPAC classification) in the range of (0.45-1.0) for P/P₀ (Figure S6). BET surface area and pore volume were 240 m²/g and 1.9 cm³/g respectively. OFG (150) exhibited narrow mesoporous pore radius in the range of 1.8 to 2.1 nm, calculated using the Barrett-Joyner-Halenda (BJH) method⁶ (inset Figure S6).

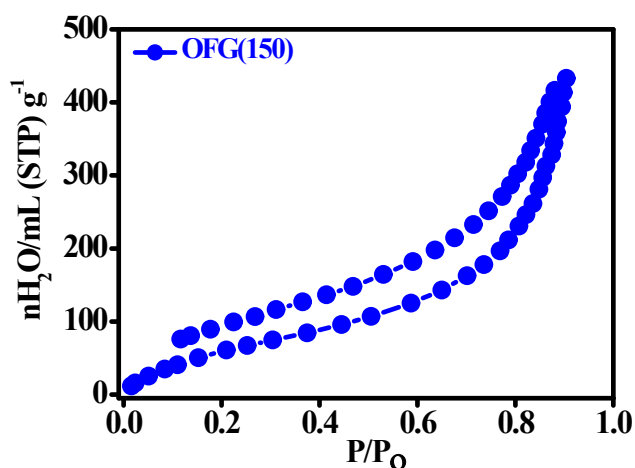


Figure S7: Pressure dependent reversible water uptake of OFG (150).

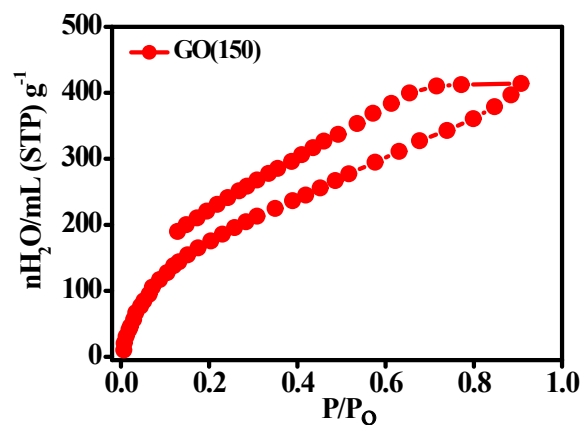


Figure S8: Pressure dependent reversible water uptake of GO (150).

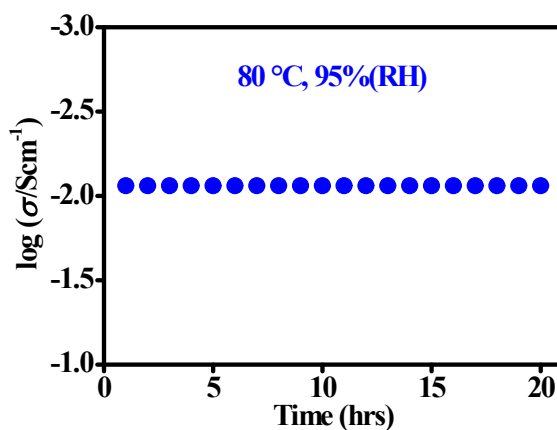


Figure S9: Time dependent proton conductivity of OFG (150) for long term stability test.

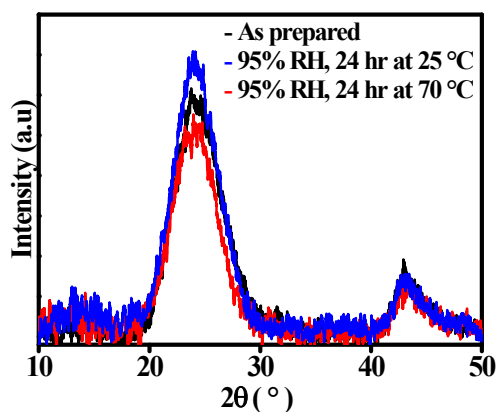


Figure S10: PXRD spectrum of OFG (150) at different conditions as mentioned in the figure.

Supercapacitor results of OFG (150):

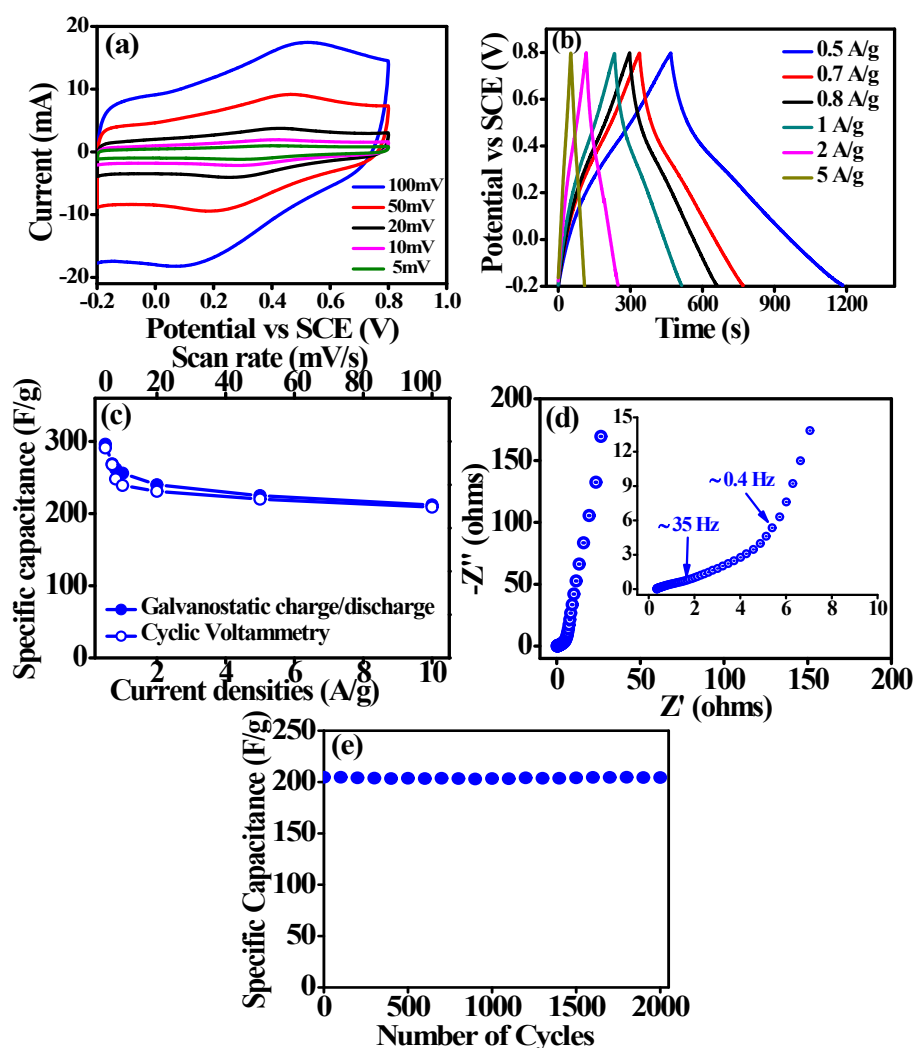


Figure S11: Electrochemical performance of OFG (150). (a) Overlap plot of CVs. (b) Overlap plot of galvanostatic charge/discharge. (c) Variation of specific capacitance with different current densities and scan rates. (d) EIS collected at 0 V versus SCE with the inset showing zoomed view of high frequency region with mass transfer frequency. (e) Cyclic stability performance at a scan rate of 50 mV/s.

Discussion related to supercapacitor study: Inspired by proton conductivity studies, we decided to explore OFG (150) as an electrochemical supercapacitor by depositing the material on a platinum (Pt) electrode using three electrodes cell in 2 M H_2SO_4 . Rectangular cyclic voltammograms (CVs) with significant pseudocapacitance (redox) contribution were obtained even at faster scan rates (Figure S11). Highest specific capacitances (C_{sp}) of 291 F/g (at 1 mV/s scan rate of CV) and 296 F/g (at 0.5 A/g current density of galvanostatic charge/discharge) were obtained (Table S5, Figures S11a, b). 68% C_{sp} retentions were obtained at high scan rate (100 mV/s) and high current density (2 A/g) (Figure S11c and Table S5). Nyquist plot of OFG (150) revealed sharp vertical rise of impedance along the imaginary axis in the low frequency region, indicating excellent capacitive nature of the materials (Figure S11d). Diffusion of electrolyte inside the material started at 35 Hz,

completed at 0.4 Hz, and thereafter complete capacitor behavior was achieved (Figure S11d, inset). Cyclic performance demonstrated 100% C_{sp} retention after 2000 cycles at 50 mV/s scan rate (Figure S11e). Excellent capacitive behavior of OFG (150) was due to following reasons. (i) hydrophilic nature of the material improved wettability and hence ion penetration,⁷ (ii) edge functionalities specially $-OH$ group improved pseudocapacitance,^{8, 9} and (iii) good electrical conductivity ensured fast electron transfer and excellent proton conductivity results in increased mass transport.⁹

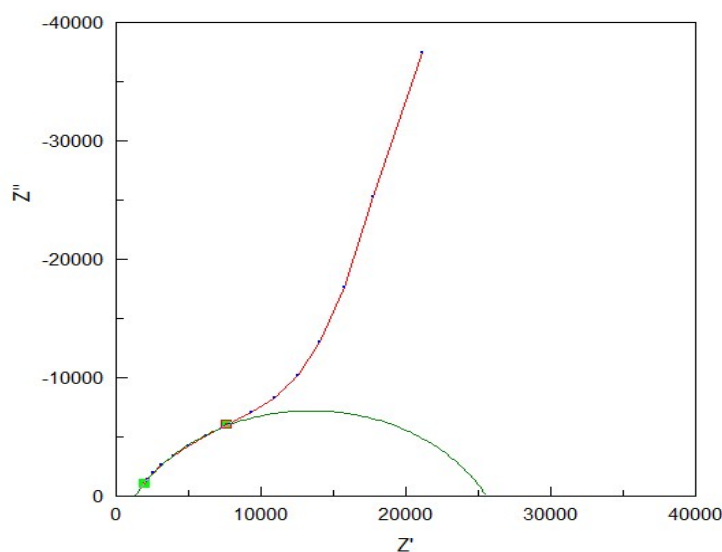


Figure S12: Fitting of EIS plot of proton conductivity measurement using Z View software.

Table S1. PXRD characteristics of graphite (150) and OFG (150).

Sample code	2θ maxima ($^{\circ}$)	$(FWHM)_{Lc}$ ($^{\circ}$)	L_c (nm)	d (\AA)	Number of layers
Graphite (150 μm)	26.4	0.19	43	3.4	126-127
OFG (150)	24.3	4.92	1.6	3.6	4-5

Table S2a. C1s peak positions and the relative atomic percentage of various functional group in OFG (150) and GO (150).

Fitting of C 1s peak Binding energy [eV] (relative atomic percentage [%])					
	C=C (sp²)	C-C/C-H (sp³)	C-O/C-O-C	C=O	O-C=O
OFG (150)	284.6 (54.5)	285.0 (26.5)	286.0 (C-O [11])	287.9 (4)	289.4 (4)
GO (150)	284.5 (32.7)	284.9 (31.3)	286.7 (21.8)	287.9 (13)	289.2 (1.2)

Table S2b. O 1s peak positions and the relative atomic percentage of various functional group in OFG (150) and GO (150).

Fitting of O 1s peak Binding energy [eV] (relative atomic percentage [%])		
	C=O	C-O/C-O-C
OFG (150)	531.1 (8)	533.1 (C-O [11])
GO (150)	531.9 (14.5)	532.8 (27)

Table S2c. Carbon and oxygen weight percentage of OFG (150) and GO (150) from XPS analysis

	Carbon (%)	Oxygen (%)	Carbon/Oxygen
OFG (150)	77	23	3.3
GO (150)	57	43	1.3

Table S3. Comparison of proton conductivity of present study with reported values of different materials

Sample	Proton conductivity (S/cm)	References
Nafion®	1×10^{-1} , (80 °C, 98% RH)	<i>J. Polym. Sci., part B: Polym. Phys.</i> , 2011, 49 , 1437.
MOF	2.1×10^{-2} , (85 °C, 90% RH)	<i>J. Am. Chem. Soc.</i> , 2013, 135 , 963.
Oxygen functionalized few-layer graphene (bulk sample)	8.7×10^{-3}, (80 °C, 95% RH)	Present work
COF (PA@Tp Azo)	9.9×10^{-4} , (25°C, 98% RH)	<i>J. Am. Chem. Soc.</i> , 2014, 136 , 6570.
Graphite oxide (200 nm, multilayer film)	4×10^{-4} , (60% RH)	<i>Angew. Chem. Int. Ed.</i> , 2014, 53 , 6997.
Graphite oxide (bulk sample)	1.3×10^{-4} , (27 °C, 98% RH)	<i>J. Am. Chem. Soc.</i> , 2013, 135 , 8097.
Zeolite (MCM-48)	3.5×10^{-5}	<i>Chem. Mater.</i> , 2008, 20 , 5122.

Table S4. Comparison of proton conductivity values (S/cm) before and after thermal annealing at 150 °C with a temperature ramp of 10 °C/min.

Sample	Before thermal annealing (70 °C, 95% RH)	After thermal annealing (70 °C, 95% RH)
OFG (150)	6.5×10^{-3}	3.9×10^{-3}
GO (150)	8.8×10^{-4}	2.2×10^{-5}

Table S5: Proton conductivity values of OFG(150) at different temperatures with 95 % RH. Pellet dimension: 6 mm diameter and thickness in the range of 1.2-1.5 mm.

Temperature (°C)	Proton conductivity x 10 ³ (S/cm)
30	0.16±0.06
50	1.5±0.4
60	1.9±0.4
70	5.9±0.8
80	8.7±0.5

Table S6. Specific capacitance (F/g) of OFG in 2 M H₂SO₄ at different scan rate of cyclic voltammetry and current densities (A/g) of galvanostatic charge/discharge.

Scan rate (mV/s)	Specific Capacitance (F/g)	Current densities (A/g)	Specific Capacitance (F/g)
100	209	10	212
50	220	5	225
20	231	2	240
10	239	1	256
5	248	0.8	262
2	268	0.7	269
1	291	0.5	296

References

1. J. H. Kang, T. Kim, J. Choi, J. Park, Y. S. Kim, M. S. Chang, H. Jung, K. T. Park, S. J. Yang and C. R. Park, *Chem. Mater.*, 2016, **28**, 756.
2. D. Yang, A. Velamakanni, G. Bozoklu, S. Park, M. Stoller, R. D. Piner, S. Stankovich, I. Jung, D. A. Field, C. A. Ventrice Jr and R. S. Ruoff, *Carbon*, 2009, **47**, 145.
3. S. Biniak, G. Szymański, J. Siedlewski and A. Świtkowski, *Carbon*, 1997, **35**, 1799.
4. R. Hawaldar, P. Merino, M. R. Correia, I. Bdikin, J. Grácio, J. Méndez, J. A. Martín-Gago and M. K. Singh, *Sci. Rep.*, 2012, **2**, 682.
5. A. C. Ferrari, *Solid State Commun.*, 2007, **143**, 47.
6. E. P. Barrett, L. G. Joyner and P. P. Halenda, *J. Am. Chem. Soc.*, 1951, **73**, 373.
7. A. J. Pak, E. Paek and G. S. Hwang, *J. Phys. Chem. C*, 2014, **118**, 21770.
8. C. Singh and A. Paul, *J. Phys. Chem. C*, 2015, **119**, 11382.
9. C. Singh, A. K. Mishra and A. Paul, *J. Mater. Chem. A*, 2015, **3**, 18557.